CORA Cork Open Research Archive
Cartlann Taighde Oscailte Chorcaí

Title	The effect of relaxation oscillations in integrated optical comb demultiplexers based on injection locking
Authors	Shortiss, Kevin;Dernaika, Mohamad;Shayesteh, Maryam;Peters, Frank H.
Publication date	2019-09-18
Original Citation	Shortiss, K., Dernaika, M., Shayesteh, M. and Peters, F. H. (2019) 'The effect of relaxation oscillations in integrated optical comb demultiplexers based on injection locking', IEEE Journal of Quantum Electronics, 55(6), pp.1-6. https://doi.org/10.1109/JQE.2019.2942053
Type of publication	Article (peer-reviewed)
Link to publisher's version	https://ieeexplore.ieee.org/document/8844062 - 10.1109/JQE.2019.2942053
Rights	© 2019, IEEE. Personal use of this material is permitted. Permission from IEEE must be obtained for all other uses, in any current or future media, including reprinting/republishing this material for advertising or promotional purposes, creating new collective works, for resale or redistribution to servers or lists, or reuse of any copyrighted component of this work in other works.
Download date	2026-11-03 09:37:33
Item downloaded from	https://hdl.handle.net/10468/8791

UCC
University College Cork, Ireland
Coláiste na hOllscoile Corcaigh

This article has been accepted for publication in a future issue of this journal, but has not been fully edited. Content may change prior to final publication. Citation information: DOI 10.1109/JQE.2019.2942053, IEEE Journal of Quantum Electronics

The Effect of Relaxation Oscillations in Integrated Optical Comb Demultiplexers based on Injection Locking

Kevin Shortiss, Mohamad Dernaika, Maryam Shayesteh, and Frank H. Peters

***Abstract*—Narrowly spaced optical combs are being considered for use in future wavelength division multiplexing optical networks. Optical injection locking has been demonstrated as an effective method of demultiplexing these narrow optical combs, and recent research has shown monolithically integrable designs can achieve side mode suppression ratios of greater than 35 dB. We present an experimental and theoretical study on how the side mode suppression ratio of these demultiplexers varies with the injected comb frequency spacing, the detuning between the slave laser and the comb, and optical injection strength. We show that the performance of these demultiplexers depends strongly on the difference between the relaxation oscillation frequency and the frequency spacing of the injected comb.**

***Index Terms*—Optical demultiplexing, injection-locked oscillator, optical comb.**

I. Introduction

WITH the continued growth of internet traffic, new optical communication infrastructures capable of dramatically increasing network bandwidth are being considered. Optical superchannels consisting of densely packed channels will be required for future networks, which could be implemented using optical frequency combs. Optical combs can increase the spectral efficiency of these superchannels by allowing the channels to be more densely packed [1]–[4], while simultaneously reducing the number of components required (decreasing the energy consumption [5]), and simplifying the digital signal processing required [6]. Flexible or elastic optical networks could provide further improvements over current wavelength division multiplexing (WDM) networks, as they allow the optical bandwidth and modulation formats used throughout the network to be dynamically adjusted to meet changing network traffic [7], [8]. Optical combs could facilitate these flexible networks, as the channel spacing [9] and modulation formats can be varied from superchannel to superchannel, to optimise the baud rates used between different nodes in the network [10], [11]. The centre frequency, of each superchannel could also be controlled using a similar method as discussed in Ref. [9].

This work was supported by Science Foundation Ireland (Grant number SFI 13/IA/1960).

K. Shortiss, M. Dernaika, M. Shayesteh and F. H. Peters are with Integrated Photonics Group, Tyndall National Institute, Cork, Ireland. (e-mail: kevin.shortiss@tyndall.ie, mohamad.dernaika@tyndall.ie, maryam.shayesteh@tyndall.ie, frank.peters@tyndall.ie).

K. Shortiss and F. H. Peters are with the Department of Physics, University College Cork, Cork, Ireland.

Manuscript received June 21, 2019; revised August 26, 2015.

However, despite these advantages, the trade-off between cost and performance must be favourable in order for optical combs to become feasible for use in future WDM networks. Integrating several components together on a photonic integrated circuit reduces both the cost and power consumption of devices, and hence recent research has been focused on creating suitable on-chip coherent optical comb transmitters [12]. For a comb based superchannel, an integrated transmitter would ideally consist of an optical comb source integrated with a demultiplexer and an array of modulators, allowing each carrier to be modulated individually, before becoming recombined and transmitted. Monolithically integrable coherent comb sources with optical comb spacings between 4 GHz and 10 GHz have already been demonstrated on InP [13]–[15], and laboratory WDM demonstrations have proven optical speeds of greater than 30 Tb/s are possible using channel spacings as narrow as 6.25 GHz [16]. Standard methods of demultiplexing these narrowly spaced optical combs on a photonic circuit are infeasible [17], as the size of arrayed waveguide grating, Echelle grating or asymmetric Mach Zehnder demultiplexers quadruples as the frequency separation between their output channels halves.

Photonic circuits which instead use optical injection locking [18]–[21] to demultiplex these narrowly spaced comb lines have been proposed as a solution to this problem [17], [22]–[26]. These demultiplexers operate by tuning the frequency of a slave laser to frequency match a line in the optical comb, causing the slave laser to injection lock to the selected comb line, amplifying [18] and demultiplexing the line [22]. As shown in Ref. [12], these demultiplexers can then be integrated with modulators to form a transmitter. This method of demultiplexing is also flexible, as the individual slave lasers can be frequency tuned to match different channels or optical comb spacings, while maintaining the fixed phase relation between the injected comb lines. Optically injecting with a frequency comb differs from the extensively studied single frequency case [18]–[21], as the comb lines which the slave laser is not locked to can still affect the slave's operation.

The side mode suppression ratio (SMSR) is often defined as the ratio of the optical power between the strongest and second strongest mode in an optical spectrum, and is a common figure of merit used to indicate the effectiveness of demultiplexers when they are integrated in a transmitter. SMSRs of greater than 37 dB at an optical comb spacing of 10 GHz have been achieved by using seperate slave lasers to lock to individual comb lines [24]. However, upon investigating the

0018-9197 (c) 2019 IEEE. Personal use is permitted, but republication/redistribution requires IEEE permission. See http://www.ieee.org/publications_standards/publications/rights/index.html for more information.

This article has been accepted for publication in a future issue of this journal, but has not been fully edited. Content may change prior to final publication. Citation information: DOI 10.1109/JQE.2019.2942053, IEEE Journal of Quantum Electronics

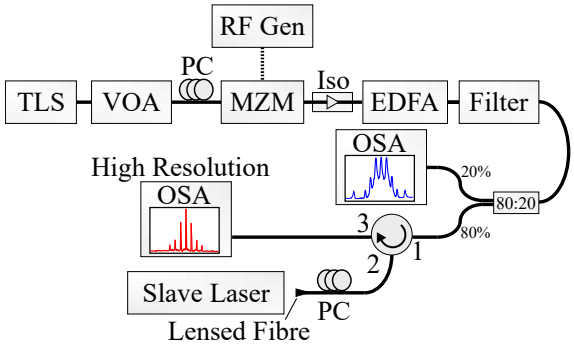


Fig. 1. Experimental setup used to investigate the SMSR obtainable. TLS: Tunable laser source, VOA: Variable optical attenuator, MZM: Mach zehnder modulator, PC: Polarisation controller, Iso: Optical isolator, EDFA: Erbium doped fibre amplifier, OSA: Optical spectrum analyser.

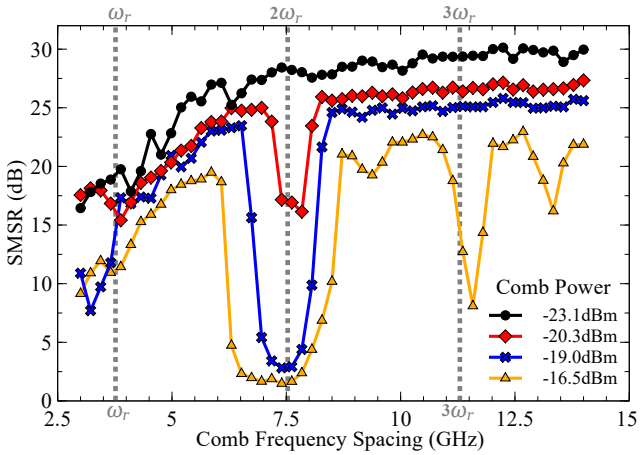


Fig. 2. Measured SMSR as the frequency spacing of the injected optical comb was varied, for four different optical injection strengths. The slave laser was maintained at current of 1.6 times threshold, at which the frequency of it's relaxation oscillations were measured to be 3.765 GHz. The free running power coupled into the lensed fibre from the slave laser was -2 dBm. Vertical gray dotted lines mark the first three multiples of the relaxation oscillation (ω_r, $2\omega_r$, and $3\omega_r$).

SMSR of devices using a theoretical model [27], we previously reported that the performance of these demultiplexers may be negatively affected as the comb frequency spacing approaches the relaxation oscillation (RO) frequency of the slave laser.

In this paper, we present an experimental and theoretical study which investigates the limits of demultiplexing optical frequency combs using injection locking. We study how the comb lines which the slave laser is not locked to affect the performance of an individual slave laser, focusing in particular on optical combs with frequency spacings close to the slave's RO frequency. We directly measure the output SMSR from a slave laser as a function of the injected comb spacing, and prove experimentally that the slave laser ROs do negatively affect the SMSR obtainable. We find that for specific frequency spacings and optical injection strengths, the ROs can become undamped, and can even become the dominant side modes in the slave laser's optical spectrum. Using our theoretical model, we simulate the optical injection of the slave laser, and find that the ROs become excited at rational fractions of the optical comb spacing. With good qualitative agreement between experiment and theory, we show that increasing the slave laser pumping can dampen the ROs enough to increase SMSR slightly, at the expense of the narrowing demultiplexer's locking bandwidth. We also calculate how the SMSR of these demultiplexers varies as a function detuning, and show that the undamped RO region originates at a slightly positive detuning, but grows into negative detunings as the injection strength is increased.

II. Experimental Results

To study how well an injection locked slave laser can demultiplex combs with narrow optical frequency spacings, experiments were performed using the setup illustrated in Fig. 1. A commercial master laser (ID Photonics CoBrite-DX1) was intensity modulated using an Oclaro LiNbO3 Mach-Zehnder modulator (MZM), to create a 3 line optical comb. The optical comb power injected into the slave laser was controlled using both a variable optical attenuator (VOA) and an erbium doped fibre amplifier (EDFA). An optical filter with a 50 GHz bandwidth at -3 dB was used to remove a portion of the amplified spontaneous emission introduced by the EDFA. Two optical spectrum analysers (OSAs) were used; a standard 2 GHz resolution OSA (Ando AQ6317B) was used to ensure there was equal power in the 3 lines of the injected optical comb, while a second 5 MHz resolution OSA (Apex AP2061A) measured the output SMSR from the slave laser. The slave laser used was an unpackaged single mode laser as described in Ref. [28], with a free running SMSR of >35 dB emitting at 1550 nm, mounted on a brass temperature controller. Optical coupling to the slave laser was achieved using a lensed fibre.

Figure 2 shows how the measured SMSR varied as the injected optical comb frequency spacing was swept from 14 GHz to 3 GHz. The slave laser's temperature was fixed such that the main lasing mode of the slave laser locked to the centre line of the three line optical comb, amplifying the centre line above the other neighbouring lines. The detuning between the slave laser and the centre line of the comb was approximately zero, and each point shows the average of 50 measurements. Four comb injection strengths are presented; for the lowest injection strength (-23.1 dBm), the SMSR decreases smoothly as the comb spacing was varied from 14 GHz to 3 GHz, dropping 14 dB in total. As shown in our previous theoretical study [27], when the optical comb frequency spacing approaches the frequency of the relaxation oscillations, the SMSR reduces significantly. The relaxation oscillation frequency ω_r of the slave laser was measured to be 3.765 GHz, and the first three multiples of ω_r are marked by grey vertical dotted lines in Fig. 2. It is known that optical injection can modify the dampening mechanism of the relaxation oscillations [19], and cause the ROs rise in optical power. The intrinsic modulation due to the relaxation oscillations adds to the frequency noise around each mode within the slave laser, and hence as the comb lines which the slave laser is not locked to approach the RO frequency, they add to the already heightened noise floor.

As the optical injection strength is increased in Fig. 2,

0018-9197 (c) 2019 IEEE. Personal use is permitted, but republication/redistribution requires IEEE permission. See http://www.ieee.org/publications_standards/publications/rights/index.html for more information.

This article has been accepted for publication in a future issue of this journal, but has not been fully edited. Content may change prior to final publication. Citation information: DOI 10.1109/JQE.2019.2942053, IEEE Journal of Quantum Electronics

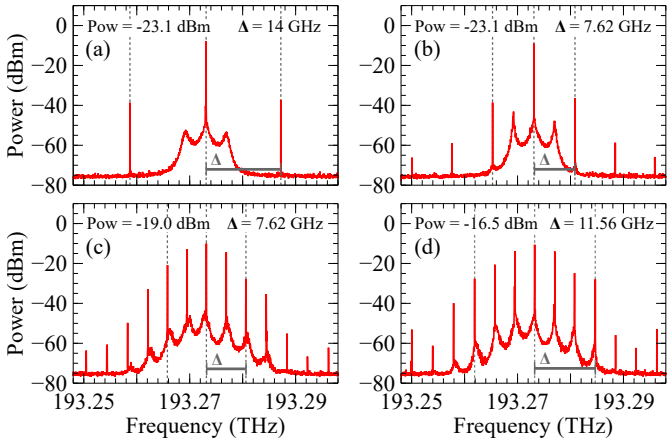


Fig. 3. Demultiplexed optical spectra, measured using an optical spectrum analyser with 5 MHz resolution. The spectra presented highlight four operating conditions with distinct behaviour. Grey vertical dotted lines indicate the frequencies of the 3 lines in the injected comb. **(a)** Injected power of −23.1 dBm, comb spacing Δ = 14 GHz: Low RO power. **(b)** Injected power of −23.1 dBm, comb spacing Δ = 7.62 GHz: ROs become undamped, rising in power. **(c)** Injected power of −19.0 dBm, comb spacing Δ = 7.62 GHz: ROs become excited, as Δ/2 approaches ω_r. **(d)** Injected power of −16.5 dBm, comb spacing Δ = 11.56 GHz: ROs become excited, as Δ/3 approaches ω_r.

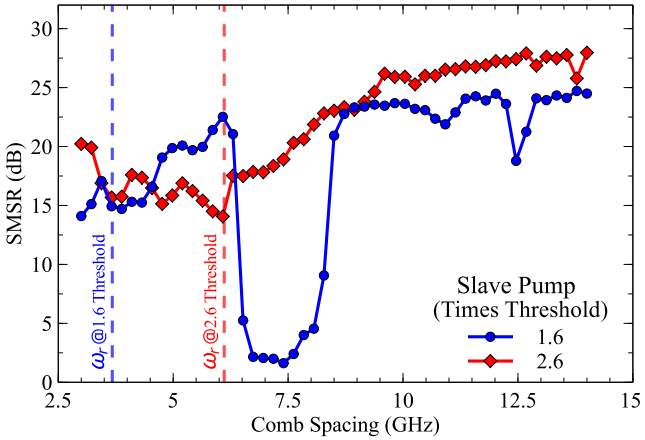


Fig. 4. Measured SMSR versus injected comb frequency spacing for pump currents of 1.6 and 2.6 times the free running laser threshold, with an injected comb power of -17.66 dBm. Vertical dotted lines show the measured RO frequency at 1.6 times (blue) and 2.6 times (red) the threshold.

we find that the SMSR decreases over all comb spacings. However, the SMSR can also be seen to dip sharply at specific comb spacings, as expected from the results in Ref. [25], [26]. However, for comb powers of -20.3 dBm (red diamonds) and -19.0 dBm (blue x's), the SMSR drops sharply at 7.5 GHz, as the comb's frequency spacing approaches $2\omega_r$. As the injection strength increases, this dip widens and the SMSR drops to only a few dB. For the highest optical injection strength presented, further decreases in the SMSR are seen, with another significant decrease occurring as the comb's frequency spacing matches $3\omega_r$, with smaller drops in performance occurring at approximately $\frac{3}{2}\omega_r$ and $\frac{5}{2}\omega_r$.

The cause of these drops in the SMSR at comb spacings of $2\omega_r$ and $3\omega_r$ is shown in Fig. 3. Different demultiplexed optical spectra are presented, indicating four different types of behaviour. In each case, grey vertical dotted lines indicate the frequencies of the 3 lines in the injected comb. Figure 3 (a) shows the slave laser output spectrum as the slave was locked to the centre line of a 14 GHz optical comb, with optical SMSR of 30 dB. The ROs in the slave (located ± 3.675 GHz from the centre line) are 40 dB lower than the lasing peak. As shown in Fig. 3 (b), the ROs become further undamped when the comb spacing is narrowed to 7.62 GHz. If the optical power is increased further, the ROs can become excited, rising higher than the sidemodes of the comb and reducing the output SMSR (as shown in Fig. 3 (c)). As the injected comb's power is increased even further, it has been found that the ROs within the slave laser can become undamped and excited whenever the injected optical comb's frequency spacing ω_r matches a multiple of the comb's frequency spacing. Demonstrated in Fig. 3 (d), the excited ROs over take the side modes in the injected optical comb, causing the SMSR to approach zero.

At larger slave laser pump currents, the frequency of the ROs increases as they also become more strongly damped. Increasing the RO damping can prevent the ROs becoming excited, and reduce the effect they have on the SMSR. Figure 4 experimentally demonstrates how increasing the slave laser pump current can benefit the SMSR obtainable. Two different slave laser pump currents were used, with a constant injected optical comb power of -17.66 dBm. The ROs still negatively affect the SMSR at comb spacings close to ω_r. However, at 2.6 times the threshold current, the RO damping in the slave laser was strong enough to prevent the slave's ROs from becoming excited and affecting the demultiplexing at higher mutliples of ω_r. For comb spacings far from the RO frequency, increasing the pump current can increase the amplification seen by the target comb line, which in turn increases the SMSR. This increase in SMSR and lack of sensitivity at multiples of ω_r comes at the expensive of the slave laser's locking bandwidth. As the locking bandwidth of the slave laser is proportional to E_i/E_0^S [21], the locking range shrinks significantly as the power in the slave laser's field grows.

III. Theoretical Model and Results

The rate equation model used to simulate the SMSR from the slave laser was as described in Ref. [20], [29]. The model assumes the slave laser's field and carriers have no spatial dependence, with the rate of change of the slave laser's electric field is given as:

$$\frac{d}{dt}\widetilde{E_s}(t) = \left(i\omega(N) + \frac{1}{2}\left[G_N(N-N_{th}) - \frac{1}{\tau_p}\right]\right)\widetilde{E_s}(t) + F_{sp} + \eta f_d \widetilde{E_M}(t), \quad (1)$$

where G_N is the laser differential gain, N_{th} is the free running threshold carrier density, τ_p is the photon lifetime within the laser cavity, η is the coupling efficiency, f_d is the longitudinal mode spacing of the slave laser, and F_{sp} describes the spontaneous emission in the laser cavity.

The change in angular optical frequency with carrier density is given as:

$$\omega(N) = \omega_0 + \frac{1}{2}\alpha G_N(N - N_{th}), \quad (2)$$

0018-9197 (c) 2019 IEEE. Personal use is permitted, but republication/redistribution requires IEEE permission. See http://www.ieee.org/publications_standards/publications/rights/index.html for more information.

This article has been accepted for publication in a future issue of this journal, but has not been fully edited. Content may change prior to final publication. Citation information: DOI 10.1109/JQE.2019.2942053, IEEE Journal of Quantum Electronics

TABLE I
PARAMETER VALUES USED IN THE MODEL.

G_N	$8.1 \times 10^{-13} m^3 s^{-1}$
ω_0	$3.798 \times 10^{14} rads^{-1}$
β	1×10^{-5}
N_{th}	$1.7172 \times 10^{24} m^{-3}$
α_H	3.5
τ_s	$1.5 \times 10^{-9} s$
τ_p	$2.0 \times 10^{-12} s$
η	1
f_d	$36 \times 10^{9} Hz$

where ω_0 is the free running angular frequency of the slave, and α is the linewidth enhancement factor. The field of the master laser $\widetilde{E_M}(t)$ which couples to the slave laser's signal was defined as in Ref. [29]:

$$\eta f_d \widetilde{E_M}(t) = \sum_j E_j e^{i\omega_j t}. \tag{3}$$

Here, E_j and ω_j are the field amplitude and angular frequency of the $j\text{-}th$ comb line.

Using the slowly varying envelope approximation, the field of the slave laser can be written as:

$$\widetilde{E_s}(t) = E_s(t) e^{i(\omega_o t + \phi_s(t))}. \tag{4}$$

Taking the derivative with respect to time of (4) and comparing it to (1) allows us to write equations explicitly for the amplitude E_s and phase ϕ_s of the slave laser's field:

$$\begin{aligned} \frac{dE_s}{dt} = &\frac{1}{2} G_N (N - N_{th}) E_s(t) \\ &+ \sqrt{\beta}\xi' + f_d \sum_j E_j \cos\left(\Delta\omega_j t - \phi_s(t)\right), \end{aligned} \tag{5}$$

$$\begin{aligned} \frac{d\phi_s}{dt} = &\frac{\alpha_H}{2} G_N (N - N_{th}) \\ &+ \sqrt{\beta}\xi'' + f_d \sum_j \frac{E_j}{E_s} \sin\left(\Delta\omega_j t - \phi_s(t)\right), \end{aligned} \tag{6}$$

where $\Delta\omega_j$ is the difference in the angular frequency of the free running laser and the $j\text{-}th$ comb line, β defines the spontaneous emission strength, and ξ' and ξ'' are the Gaussian white noise source terms which contribute to the spontaneous emission term F_{sp}. The real and imaginary parts ξ' and ξ'' of the noise fulfill the conditions $\langle \xi'(t)\xi'(t') \rangle = \langle \xi''(t)\xi''(t') \rangle = \delta(t - t')$, and $\langle \xi'(t)\xi''(t') \rangle = 0$. The rate of change of carriers for a pump rate R_p was given as:

$$\frac{dN}{dt} = R_p - \frac{N}{\tau_s} - G_N (N - N_{th}) E_s(t)^2 - \frac{1}{\tau_p} E_s(t)^2. \tag{7}$$

For the above rate equations, the free running steady state electric field E_0^S and the relaxation oscillation frequency ω_r are given by [20] :

$$E_0^S = \sqrt{\tau_p \left(R_p - \frac{N_{th}}{\tau_s} \right)}, \tag{8}$$

$$\omega_r = \sqrt{G_N \left(R_p - \frac{N_{th}}{\tau_s} \right)}. \tag{9}$$

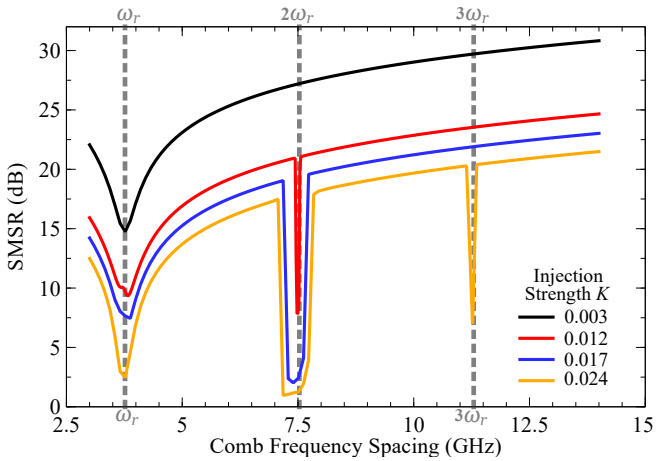


Fig. 5. Calculated SMSR as the frequency spacing of the injected optical comb was varied, for four different optical injection strengths. The optical injection strength K was defined as in Ref. [21], with $K = f_d E_i / \omega_r E_0^S$. The slave laser was fixed at 1.6 times it's threshold, at which the frequency of it's relaxation oscillations was 3.765 GHz. Vertical gray dotted lines mark the first three multiples of the relaxation oscillation (ω_r, $2\omega_r$, and $3\omega_r$).

Approximate values for N_{th}, G_N and τ_s were found by fitting measured values of the slave laser's free running relaxation oscillation frequency. All parameters values used in the model, unless otherwise stated, are presented in Table I.

Our model was then used to simulate the experimental results presented in Fig. 2. A fourth order Runge-Kutta method [30] was implemented to solve the rate equations. A numerical time step of 2.56 ps was used, and the slave laser was allowed to reach steady state prior to optical injection. Data collection started 1 μs after the optical injection, and was recorded over a simulation time of 150 μs. This provided a frequency resolution of 6.7 KHz. The calculated results for how the comb frequency spacing affected the SMSR is shown in Fig. 5. There is good qualitative agreement between theory and experiment; as the experimental results indicated, the SMSR decreases as the injected power is increased. The calculated SMSR declines as the comb spacing was varied from 14 GHz to the relaxation frequency ω_r, however after the reaching the relaxation oscillation frequency, the SMSR can be seen to increase again. This could be due in part to unrealistic modelling of the ROs; the measured device ROs span a wider frequency range than in the calculated results. This is also likely the cause of the discrepancy between the widths of the regions where the ROs have become excited, as these regions appear larger in experiment than in theory. However, good agreement is still seen, as at higher powers the model also predicts drops in the performance at frequency spacings close to ω_r, $2\omega_r$ and $3\omega_r$, as seen in experiment.

From the simulations, we find that the comb lines which the slave laser is not locked to can modulate the slave laser's field at a frequency corresponding to the comb's frequency spacing. When this extra modulation frequency becomes resonant with the natural RO frequency (or a harmonic of the RO frequency), the ROs undampen and rise in power.

The theoretical results also show that the large drops in SMSR at specific comb frequency spacings can be avoided by

0018-9197 (c) 2019 IEEE. Personal use is permitted, but republication/redistribution requires IEEE permission. See http://www.ieee.org/publications_standards/publications/rights/index.html for more information.

This article has been accepted for publication in a future issue of this journal, but has not been fully edited. Content may change prior to final publication. Citation information: DOI 10.1109/JQE.2019.2942053, IEEE Journal of Quantum Electronics

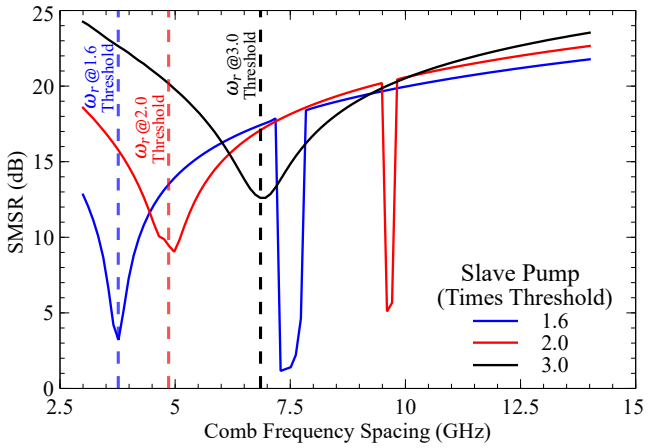


Fig. 6. Calculated SMSR versus injected comb frequency spacing for pump currents of 1.6, 2.0 and 3.0 times the free running laser threshold, with an injected comb strength $K = 0.023$. As the pump current is increased, the relaxation oscillations frequency increases. Vertical dotted lines show the measured RO frequency at 1.6 times (blue), 2.0 times (red) and 3.0 times (black) the threshold.

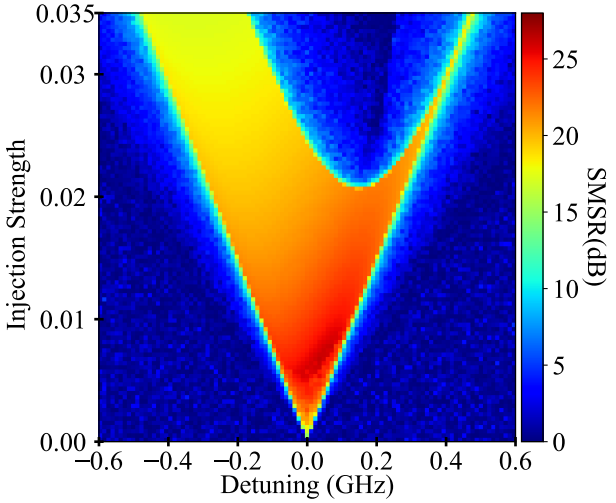


Fig. 7. Intensity plot showing how the SMSR varies as the detuning and comb injection power is varied, for a comb spacing of 10 GHz, and slave laser drive current at 1.6 times threshold. The optical injection strength K was defined as in Ref. [21], with $K = f_d E_i/\omega_r E_0^S$.

increasing the slave laser's pump current. As shown in Fig. 6, increasing the pump current from 1.6 times threshold to 3.0 times threshold stops the ROs becoming excited. The model predicts that the dip in the SMSR for comb spacings equal to ω_r becomes wider and shallower as the pump current is increased. In comparison, the SMSR at ω_r was approximately the same for both pump currents shown in Fig. 4. The dip due to the ROs at comb spacings close to ω_r is also much less pronounced in experiment than in the theoretical results, indicating that possibly a more accurate description of the carrier's rate equation could be required. The model also omits any roll off in the laser's gain as the current is increased, and we expect that as laser gain clamps, further increasing the optical pumping will also lead to a degradation in SMSR.

Finally, we present how the detuning between the slave and the centre line of the comb affects the SMSR. Figure 7 shows an intensity plot of the parameter space spanned by optical injection strength and the detuning between the centre comb line and the slave laser. High SMSR indicates the regions over which the slave is frequency locked to the comb. At lower injection strengths the SMSR is symmetric around zero detuning [26], and as the injection strength increases, the peak SMSR appears instead at slightly positive detunings. The locking bandwidth grows as expected with increasing injection strength, however slightly above an injection strength of K = 0.02, the SMSR is seen to drop to zero within the cone-shapped locked region in Fig. 7. This low SMSR region is caused by the ROs becoming undamped and excited [19]. The undamped RO region originates at a slightly positive detuning, but grows into negative detunings as the injection strength is increased. As higher SMSRs also predominantly occur at lower injection strengths, operating at lower injection strengths is favourable.

IV. Conclusion

A detailed study of the constraints of demultiplexing an optical comb using an injection locked slave has been presented. We have shown, using both experimental and simulated results that the SMSR decreases as the frequency spacing of the comb's lines approaches the relaxation oscillation in the slave laser. In addition, it was shown that for specific frequency spacings and optical injection strengths, the ROs can become undamped, and can even become the dominant side modes in the slave laser's optical spectrum, causing the output SMSR to approach zero in some cases. Increasing the slave laser drive current can improve the SMSR for specific comb spacings, at the expense of a reduced locking bandwidth. Using our model, we show how detuning and optical injected strength effects the output SMSR, and find that the ROs initially become undamped and perturb the demultiplexing at positive detunings from the centre comb line.

Our results show the output SMSR and the locking bandwidth of the slave laser are inversely proportional. Hence, optimal SMSR will always be achieved when the slave laser is very weakly locked to the master. By integrating both the optical comb source and demultiplexer on a photonic circuit, one can minimise losses and reduce the effects of thermal drift on the comb-slave system. This will require an integration technique which does not affect the individual performance of the comb source or the array of slave lasers in the demultiplexer.

Acknowledgment

The authors would like to thank Science Foundation Ireland for funding this research, under award SFI 13/IA/1960.

References

[1] A. Ellis and F. Gunning, "Spectral density enhancement using coherent WDM," *IEEE Photonics Technology Letters*, vol. 17, no. 2, pp. 504–506, feb 2005. [Online]. Available: http://ieeexplore.ieee.org/document/1386363/

[2] P. M. Anandarajah, M. Deseada Gutierrez Pascual, S. O'Duill, J. Bradell, F. Smyth, and P. Landais, "Integrated frequency combs for flexible optical networks," in *2017 Photonics North (PN)*. IEEE, jun 2017, pp. 1–1. [Online]. Available: http://ieeexplore.ieee.org/document/8090555/

0018-9197 (c) 2019 IEEE. Personal use is permitted, but republication/redistribution requires IEEE permission. See http://www.ieee.org/publications_standards/publications/rights/index.html for more information.

This article has been accepted for publication in a future issue of this journal, but has not been fully edited. Content may change prior to final publication. Citation information: DOI 10.1109/JQE.2019.2942053, IEEE Journal of Quantum Electronics

[3] M. Mazur, A. Lorences-Riesgo, J. Schroder, P. A. Andrekson, and M. Karlsson, "10 Tb/s PM-64QAM Self-Homodyne Comb-Based Superchannel Transmission With 4% Shared Pilot Tone Overhead," *Journal of Lightwave Technology*, vol. 36, no. 16, pp. 3176–3184, aug 2018. [Online]. Available: https://ieeexplore.ieee.org/document/8327487/

[4] V. Torres-Company, J. Schröder, A. Fülöp, M. Mazur, L. Lundberg, Ó. B. Helgason, M. Karlsson, and P. A. Andrekson, "Laser Frequency Combs for Coherent Optical Communications," *J. Lightwave Technol.*, vol. 37, no. 7, pp. 1663–1670, apr 2019. [Online]. Available: http://jlt.osa.org/abstract.cfm?URI=jlt-37-7-1663

[5] D. J. Blumenthal, "Integrated combs drive extreme data rates," *Nature Photonics*, vol. 12, no. 8, pp. 447–450, aug 2018. [Online]. Available: http://www.nature.com/articles/s41566-018-0222-4

[6] L. Lundberg, M. Karlsson, A. Lorences-Riesgo, M. Mazur, V. Torres-Company, J. Schröder, P. Andrekson, L. Lundberg, M. Karlsson, A. Lorences-Riesgo, M. Mazur, V. Torres-Company, J. Schröder, and P. A. Andrekson, "Frequency Comb-Based WDM Transmission Systems Enabling Joint Signal Processing," *Applied Sciences*, vol. 8, no. 5, p. 718, may 2018. [Online]. Available: http://www.mdpi.com/2076-3417/8/5/718

[7] I. Tomkos, S. Azodolmolky, J. Sole-Pareta, D. Careglio, and E. Palkopoulou, "A tutorial on the flexible optical networking paradigm: State of the art, trends, and research challenges," *Proceedings of the IEEE*, vol. 102, no. 9, pp. 1317–1337, sep 2014. [Online]. Available: http://ieeexplore.ieee.org/document/6824237/

[8] G. Zhang, M. De Leenheer, A. Morea, and B. Mukherjee, "A Survey on OFDM-Based Elastic Core Optical Networking," *IEEE Communications Surveys & Tutorials*, vol. 15, no. 1, pp. 65–87, 2013. [Online]. Available: http://ieeexplore.ieee.org/document/6148192/

[9] M. D. G. Pascual, R. Zhou, F. Smyth, P. M. Anandarajah, and L. P. Barry, "Software reconfigurable highly flexible gain switched optical frequency comb source," *Optics Express*, vol. 23, no. 18, p. 23225, sep 2015. [Online]. Available: https://www.osapublishing.org/abstract.cfm?URI=oe-23-18-23225

[10] T. Zami, "Co-Optimizing Allocation of Nyquist Superchannels and Physical Impairments Aware Placement of Regenerators in Elastic WDM Networks," *Journal of Lightwave Technology, Vol. 32, Issue 16, pp. 2830-2840*, vol. 32, no. 16, pp. 2830–2840, aug 2014. [Online]. Available: https://www.osapublishing.org/jlt/abstract.cfm?uri=jlt-32-16-2830

[11] M. Klinkowski, M. Ruiz, L. Velasco, D. Careglio, V. Lopez, and J. Comellas, "Elastic Spectrum Allocation for Time-Varying Traffic in FlexGrid Optical Networks," *IEEE Journal on Selected Areas in Communications*, vol. 31, no. 1, pp. 26–38, jan 2013. [Online]. Available: http://ieeexplore.ieee.org/document/6381741/

[12] N. P. Kelly, M. Dernaika, L. Caro, P. E. Morrissey, and F. H. Peters, "Monolithic Integration of Photonic Devices for Use in a Regrowth-Free CoWDM Transmitter," *IEEE Photonics Technology Letters*, vol. 29, no. 12, pp. 941–944, jun 2017. [Online]. Available: http://ieeexplore.ieee.org/document/7919190/

[13] J. K. Alexander, P. E. Morrissey, H. Yang, M. Yang, P. J. Marraccini, B. Corbett, and F. H. Peters, "Monolithically integrated low linewidth comb source using gain switched slotted Fabry-Perot lasers," *Optics Express*, vol. 24, no. 8, p. 7960, apr 2016. [Online]. Available: https://www.osapublishing.org/abstract.cfm?URI=oe-24-8-7960

[14] M. D. G. Pascual, V. Vujicic, J. Braddell, F. Smyth, P. Anandarajah, and L. Barry, "Photonic Integrated Gain Switched Optical Frequency Comb for Spectrally Efficient Optical Transmission Systems," *IEEE Photonics Journal*, vol. 9, no. 3, pp. 1–8, jun 2017. [Online]. Available: http://ieeexplore.ieee.org/document/7915677/

[15] M. N. Hammad, E. P. Martin, P. D. Lakshmijayasimha, A. Kaszubowska-Anandarajah, P. Landais, and P. M. Anandarajah, "Optimum optical frequency comb generation via externally injection of a gain switched VCSEL," in *Conference on Lasers and Electro-Optics*. Washington, D.C.: OSA, may 2019, p. SM4N.6. [Online]. Available: https://www.osapublishing.org/abstract.cfm?URI=CLEO{_}SI-2019-SM4N.6

[16] V. Ataie, E. Temprana, L. Liu, E. Myslivets, B. P.-P. Kuo, N. Alic, and S. Radic, "Flex-grid Compatible Ultra Wide Frequency Comb Source for 31.8 Tb/s Coherent Transmission of 1520 UDWDM Channels," in *Optical Fiber Communication Conference: Postdeadline Papers*. Washington, D.C.: OSA, 2014, p. Th5B.7. [Online]. Available: https://www.osapublishing.org/abstract.cfm?URI=OFC-2014-Th5B.7

[17] W. Cotter, P. E. Morrissey, H. Yang, J. O'Callaghan, B. Roycroft, B. Corbett, and F. H. Peters, "Integrated demultiplexing and amplification of coherent optical combs," *Optics Express*, vol. 27, no. 11, p. 16012, may 2019. [Online]. Available: https://www.osapublishing.org/abstract.cfm?URI=oe-27-11-16012

[18] R. Lang, "Injection locking properties of a semiconductor laser," *IEEE Journal of Quantum Electronics*, vol. 18, no. 6, pp. 976–983, jun 1982. [Online]. Available: http://ieeexplore.ieee.org/document/1071632/

[19] I. Petitbon, P. Gallion, G. Debarge, and C. Chabran, "Locking bandwidth and relaxation oscillations of an injection-locked semiconductor laser," *IEEE Journal of Quantum Electronics*, vol. 24, no. 2, pp. 148–154, feb 1988. [Online]. Available: http://ieeexplore.ieee.org/document/108/

[20] F. Mogensen, H. Olesen, and G. Jacobsen, "Locking conditions and stability properties for a semiconductor laser with external light injection," *IEEE Journal of Quantum Electronics*, vol. 21, no. 7, pp. 784–793, jul 1985. [Online]. Available: http://ieeexplore.ieee.org/document/1072760/

[21] S. Wieczorek, B. Krauskopf, T. Simpson, and D. Lenstra, "The dynamical complexity of optically injected semiconductor lasers," *Physics Reports*, vol. 416, no. 1-2, pp. 1–128, sep 2005. [Online]. Available: https://www.sciencedirect.com/science/article/pii/S0370157305002656

[22] W. E. Cotter, D. Goulding, B. Roycroft, J. O'Callaghan, B. Corbett, and F. H. Peters, "Investigation of active filter using injection-locked slotted FabryPerot semiconductor laser," *Applied Optics*, vol. 51, no. 30, p. 7357, oct 2012. [Online]. Available: https://www.osapublishing.org/abstract.cfm?URI=ao-51-30-7357

[23] A. C. Bordonalli, M. J. Fice, and A. J. Seeds, "Optical injection locking to optical frequency combs for superchannel coherent detection," *Optics Express*, vol. 23, no. 2, p. 1547, jan 2015. [Online]. Available: https://www.osapublishing.org/abstract.cfm?URI=oe-23-2-1547

[24] M. D. Gutierrez, J. Braddell, F. Smyth, and L. P. Barry, "Monolithically integrated 1x4 comb de-multiplexer based on injection locking," in *European Conf. Integrated Optics*, 2016, pp. 1–2.

[25] S. P. Ó Duill, P. M. Anandarajah, F. Smyth, L. P. Barry, A. J. Seeds, S. V. Chernikov, M. J. Guy, J. R. Taylor, and A. S. Siddiqui, "Injection-locking criteria for simultaneously locking single-mode lasers to optical frequency combs from gain-switched lasers," in *IEEE J. Quantum Electron*, B. Witzigmann, M. Osiński, and Y. Arakawa, Eds., vol. 18, no. 6. International Society for Optics and Photonics, feb 2017, p. 100980H. [Online]. Available: http://proceedings.spiedigitallibrary.org/proceeding.aspx?doi=10.1117/12.2249769

[26] P. D. Lakshmijayasimha, E. P. Martin, S. P. Ó Duill, P. Landais, P. M. Anandarajah, and A. Kaszubowska-Anandarajah, "Performance of an injection-locked active demultiplexer for FSR-tunable optical frequency combs," in *Conference on Lasers and Electro-Optics*. Washington, D.C.: OSA, may 2019, p. STu4N.5. [Online]. Available: https://www.osapublishing.org/abstract.cfm?URI=CLEO{_}SI-2019-STu4N.5

[27] K. J. Shortiss, M. Shayesteh, and F. H. Peters, "Modelling the effect of slave laser gain and frequency comb spacing on the selective amplification of injection locked semiconductor lasers," *Optical and Quantum Electronics*, vol. 50, no. 1, p. 49, jan 2018. [Online]. Available: http://link.springer.com/10.1007/s11082-018-1317-3

[28] K. Shortiss, M. Dernaika, L. Caro, M. Seifikar, and F. H. Peters, "Inverse Scattering Method Design of Regrowth-Free Single-Mode Semiconductor Lasers Using Pit Perturbations for Monolithic Integration," *IEEE Photonics Journal*, vol. 10, no. 5, pp. 1–10, oct 2018. [Online]. Available: https://ieeexplore.ieee.org/document/8477050/

[29] D. S. Wu, D. J. Richardson, and R. Slavik, "Selective amplification of frequency comb modes via optical injection locking of a semiconductor laser: influence of adjacent unlocked comb modes," in *Proc. SPIE 8781, Integrated Optics: Physics and Simulations*, may 2013, p. 87810J. [Online]. Available: http://proceedings.spiedigitallibrary.org/proceeding.aspx?doi=10.1117/12.2017371

[30] W. H. Press, W. T. Vetterling, S. A. Teukolsky, and B. P. Flannery, *Numerical recipes in C++ : the art of scientific computing*. Cambridge University Press, 2002. [Online]. Available: https://dl.acm.org/citation.cfm?id=506164

Kevin Shortiss received the B. Sc. degree in physics and mathematics from University College Cork in 2015. He is currently pursuing the Ph. D. degree in photonic integrated optical demultiplexers, with the integrated photonics group, Tyndall National Institute, Cork, Ireland. His current research interests include optical injection, optical demultiplexing, and semiconductor ring lasers.

0018-9197 (c) 2019 IEEE. Personal use is permitted, but republication/redistribution requires IEEE permission. See http://www.ieee.org/publications_standards/publications/rights/index.html for more information.

This article has been accepted for publication in a future issue of this journal, but has not been fully edited. Content may change prior to final publication. Citation information: DOI 10.1109/JQE.2019.2942053, IEEE Journal of Quantum Electronics

Mohamad Dernaika is currently a senior design engineer InP technologies at Rockley Photonics. In 2019, he received his PhD from University College Cork and with the Integrated Photonic Group, Tyndall National Institute. He received his masters degree in broadband telecommunication networks from the University of Hertfordshire in 2011. Between 2013 and 2015, he worked as a researcher in ultrafast fiber lasers with Photonic Research Center, Malaya University. His research interests include semiconductor lasers, photonic integrated circuits, micro transfer printing, injection locked lasers, and monolithic integration.

Maryam Shayesteh is currently a postdoctoral researcher in Integrated Photonics Group at Tyndall National Institute, University College Cork, Ireland. She received her PhD in Micro-Nano electronics in 2014 . Since then she has been working on InP-based solar cells and integrated photonic circuits. Her research interests are device design, fabrication and characterization.

Frank H. Peters (M'96) was born in Victoria, BC, Canada. He received the B.Eng. degree in engineering physics from the Technical University of Nova Scotia, Canada, in 1988, and the Ph.D. degree from McMaster University, Hamilton, ON, Canada, in 1991. From 1991 to 1993, he worked as a Research Engineer with the Electrical and Computer Engineering Department, University of California, Santa Barbara, CA, USA. From 1993 until 2001, he worked as a Research Scientist with Optical Concepts, W. L. Gore, and Associates and Agilent Technologies developing and integrating photonic devices into datacom and telecom applications. From 2001 to 2005, he was with Infinera in Sunnyvale California working in the development of high-speed photonic integrated circuits, and then moved to Ireland in 2005. He is currently a Professor with the Physics Department. University College Cork, Cork, Ireland and the Head of the Integrated Photonics group with the Tyndall National Institute, Cork, Ireland. He has authored more than 200 papers and holds more than 40 patents all concerned with thermal, optical, electrical and systems issues relating to the design and use of photonic devices and high speed photonic integrated circuits.

0018-9197 (c) 2019 IEEE. Personal use is permitted, but republication/redistribution requires IEEE permission. See http://www.ieee.org/publications_standards/publications/rights/index.html for more information.